Chemical Engineering Journal 158 (2010) 489–497

Contents lists available at ScienceDirect

Chemical Engineering Journal

journal homepage: www.elsevier.com/locate/cej

Equilibrium, thermodynamics and process design to minimize adsorbent amount for the adsorption of acid dyes onto cationic polymer-loaded bentonite

Qian Li[a,b], Qin-Yan Yue[a,*], Yuan Su[c], Bao-Yu Gao[a], Hong-Jian Sun[b]

[a] Shandong Key Laboratory of Water Pollution Control and Resource Reuse, School of Environmental Science and Engineering, Shandong University, No. 27 Shanda South Road, Shandong, Jinan, 250100, PR China
[b] School of Chemistry and Chemical Engineering, Shandong University, Jinan, 250100, PR China
[c] Department of Mathematics and Statistics, Shandong Economic University, Jinan, 250014, PR China

ARTICLE INFO

Article history:
Received 20 October 2009
Received in revised form 17 January 2010
Accepted 18 January 2010

Keywords:
Acid dye
Cationic polymer/bentonite
Adsorption equilibrium
Thermodynamics
Process design

ABSTRACT

The adsorption equilibrium, thermodynamics and process design of the polyepicholorohydrin-dimethylamine (EPI-DMA) cationic polymer-loaded bentonite (EPI-DMA/bentonite) for the removal of two acid dyes (Acid Scarlet GR and Acid Dark Blue 2G) were studied to assess the adsorption capacities, mechanisms and the minimum adsorbent amount. The effects of solution pH and salt concentration on the removal of acid dye were also investigated. The equilibrium data were analyzed by the Langmuir and Freundlich model, which revealed that Freundlich model was more suitable to describe the acid dyes adsorption than Langmuir model. According to the dependence of thermodynamic equilibrium constant (K_s) on temperatures, the thermodynamic parameters associated with the adsorption process were calculated. The negative values of ΔG^0 indicate that the overall adsorption processes are spontaneous. And the positive values of ΔH^0 show that the adsorption processes are endothermic in nature and the adsorption mechanisms are between physical adsorption and chemisorption. Based on the well correlated adsorption isotherm, an adsorption process design model has been developed for the design of a two-stage batch adsorber to predict the minimum amount of adsorbent to achieve a specified percentage of dye removal. Results show that compared with the single-stage batch adsorption, the two-stage process can significantly save adsorbent to meet the needs for higher dye removal efficiency (>99%) and therefore minimize capital investment costs.

1. Introduction

Adsorption as an effective method for contaminant treatment appears to offer the best potential for color removal. In recent years, many alternative technologies and potential adsorbents have been tried for dye-bearing wastewater treatment, including clay and clay minerals, peat, wood, and alunite [1–6]. Bentonite is a clay mineral, which is mainly composed of montmorillonite. It is a 2:1 type aluminosilicate, the unit layer structure of which consists of one $A1^{3+}$ octahedral sheet placed between two Si^{4+} tetrahedral sheets. Replacing the exchangeable inorganic cations (e.g. Na^+, Ca^{2+}, H^+) on the internal and external surfaces of montmorillonite with organic cations, such as quaternary ammonium salt surfactants [7–10], enhances the adsorption capacity as the bentonite surfaces change from hydrophilic to hydrophobic [7]. Therefore, organophilic bentonite becomes an excellent adsorbent for organic pollutants, such as dye molecules [9–11].

Cationic polymers, which comprise organic cations containing nonpolar groups, are suitable for rendering clays less polar and hence more hydrophobic. And compared with traditional organobentonites, cationic polymer-loaded bentonites involve much lower cost and can avoid secondary pollution caused by the surfactants desorption, especially when the cationic polymers have been widely applied in wastewater treatment. As it is a novel class of adsorbent, the preparation of cationic polymer/bentonite and the adsorption properties for the removal of anionic and non-ionic organic pollutants from wastewater have been investigated by several researchers [12–14]. Recently, with the in-depth study of polymer/bentonite as adsorbent, several researchers begin to investigate the application of novel polymer/bentonite complexes for dye removal [15,16]. Polyepicholorohydrin-dimethylamine (EPI-DMA), a water-soluble cationic polyelectrolyte with amido-cyanogen and ammonium functional groups, has been successfully applied in the treatment of printing and dyeing wastewater and also been proved to have the potential to render bentonite suitable for the removal of organic contaminants [17–19]. In our previous study, the cationic polymer EPI-DMA loaded bentonite, namely EPI-DMA/bentonite, has been prepared successfully and it has also been verified that EPI-DMA/bentonite possesses good adsorption prop-

* Corresponding author. Tel.: +86 531 88365258; fax: +86 531 88364832.
E-mail address: qyyue58@yahoo.com.cn (Q.-Y. Yue).

1385-8947/$ – see front matter © 2010 Elsevier B.V. All rights reserved.
doi:10.1016/j.cej.2010.01.033

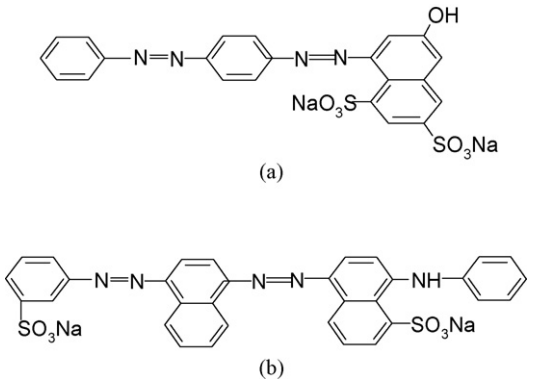

Fig. 1. Chemical structures of two acid dyes: (a) AS GR and (b) ADB 2G.

erty so as be potential adsorbents for organic pollutants especially for dyes [20,21].

As an important kind of water-soluble anionic dyes, acid dyes are brightly colored and widely applied to dyeing nylon, wool, silk and so on. However, only a few studies have been carried out to investigate the adsorption of acid dyes onto activated clays [9,22], and recently a few researchers start to pay attention to the adsorption properties of acid dyes onto cationic polymer-loaded bentonite [16,23]. As a new cationic polymer-loaded bentonite, EPI-DMA/bentonite could potentially be a good adsorbent for acid dye removal. So, the study of adsorption property of acid dyes onto EPI-DMA/bentonite is necessary.

For the adsorbent, the required adsorbent amount is directly related to the cost, which can be evaluated according to the adsorption capacity by equilibrium adsorption [24]. However, the previous studies mostly focused on the determination of adsorbent capacity, thermodynamic parameters, influences of operating parameters and so on [25–29]. The application of these data in adsorption process design such as batch adsorber design for pollutant removal was limited. Moreover, the limited application of optimization models was mostly based on a single-stage batch adsorber design to predict the amount of adsorbent required to remove a certain amount of pollutant from a fixed volume of wastewater [24,30,31], and gave little consideration to other process design to minimize adsorbent amount.

In the present study, the adsorption properties of EPI-DMA/bentonite for two acid dyes, namely Acid Scarlet (AS GR) and Acid Dark Blue 2G (ADB 2G), have been studied. The equilibrium isotherms and thermodynamics have been investigated to determine the adsorption capacities and the adsorption mechanisms. Based on the equilibrium studies, this paper develops a multi-stage batch adsorber design model. A design analysis method has been used to predict the minimum amount of adsorbent required to achieve a specific dye removal percentage at a given volume of wastewater effluents in the two-stage batch adsorber adsorption process. The minimum amount of adsorbent required maximizes the efficiency of adsorbent and therefore reduces capital investment costs.

2. Materials and methods

2.1. Materials

The acid dyes used in the experiments were supplied by Binzhou Dye Printing Co. (Shandong, China), which were Acid Scarlet (AS GR) and Acid Dark Blue 2G (ADB 2G). The chemical structures of the dyes are depicted in Fig. 1. All these dyes were of commercial grade and were used without further purification.

The bentonite to prepare EPI-DMA/bentonite was provided from the city of Weifang, Shandong, China. The cation exchange capacity (CEC) of the clay, measured by the methylene blue method, was 700 mmol/kg. The cationic polyelectrolyte polyepicholorohydrin-dimethylamine (EPI-DMA) applied to modify bentonite was produced by Binzhou Chemical Co. (Shandong, China), which had a viscosity of 400 mPa/s, a cationic degree of 3.6 mmol/g.

To obtain a complex containing a given content of cationic polymer, a dispersion of 2.0 g oven-dried bentonite in 90 mL deionized water was first prepared. Then 10 mL of an aqueous EPI-DMA solution was introduced to make the final EPI-DMA solution concentration equal to 8.0 g L^{-1} and the mixture was shaken end-over-end on a temperature-controlled shaker at the desired temperature of 40 °C for 2 h. The complex was separated from the mixture by vacuum filtering and washed several times with deionized water. The cationic polymer–bentonite complex was dried at 60 °C in an oven and activated for 1 h at 105 °C, and then stored for further use. This bentonite is designated as EPI-DMA/bentonite [19]. The present EPI-DMA/bentonite contains EPI-DMA polymer 92.5 mg/(g clay), possesses a net positive charge of +10.12 mV, and is more hydrophobic according to our previous TG-DSC analysis [19]. Other properties of EPI-DMA/bentonite are also characterized by XRD and FTIR analysis.

2.2. Characteristics of the materials

The raw bentonite and EPI-DMA/bentonite were analyzed by X-ray powder diffraction using a D/max-RB diffractometer with CuKα radiation.

The contents of carbon and nitrogen in raw bentonite and EPI-DMA/bentonite, respectively, were measured by element analyzer (Elementar Vario EL III, Germany) to determine the C/N ratio.

FTIR spectra for raw bentonite and EPI-DMA/bentonite were recorded (KBr) on a FT/IR-20SX Model Fourier transform infrared spectrometer to confirm the modification.

2.3. Adsorption experiments

The adsorption experiments were carried out by using a sample containing 0.2 g of EPI-DMA/bentonite and 100 mL of dye solution in 250 mL flasks and shaking on a horizontal shaker. The solution initial pH value, which was 7.5 for AS GR and 7.9 for ADB 2G, respectively, was used throughout all adsorption experiments, except when the effect of solution pH was examined. The salt concentration value used throughout the adsorption experiments was 0 M, except when the effect of salt concentration was examined. The adsorption experiments were performed at various initial concentrations (0–100 mg/L) for 120 min at three temperatures (293, 303 and 313 K), respectively, to allow attainment of equilibrium to determine the adsorption equilibrium isotherms and the maximum adsorption amount of dye. The solution was filtered and then analyzed quantitatively. The dye concentration in the clear supernatant was then determined by spectrophotometric method. All measurements were recorded at the wavelength corresponding to maximum absorbance, λ_{max}, which was 508 nm for AS GR and 636 nm for ADB 2G, respectively, using spectrophotometer (UV-754). The reproducibility during concentration measurements was ensured by repeating the experiments three times under identical conditions and the average values were calculated. Standard deviations of experiments were found to be within ±3.0%. The amount of adsorbed dye, Q (mg/g), under different conditions was calculated by

$$Q = \frac{V(C_0 - C_e)}{W} \quad (1)$$

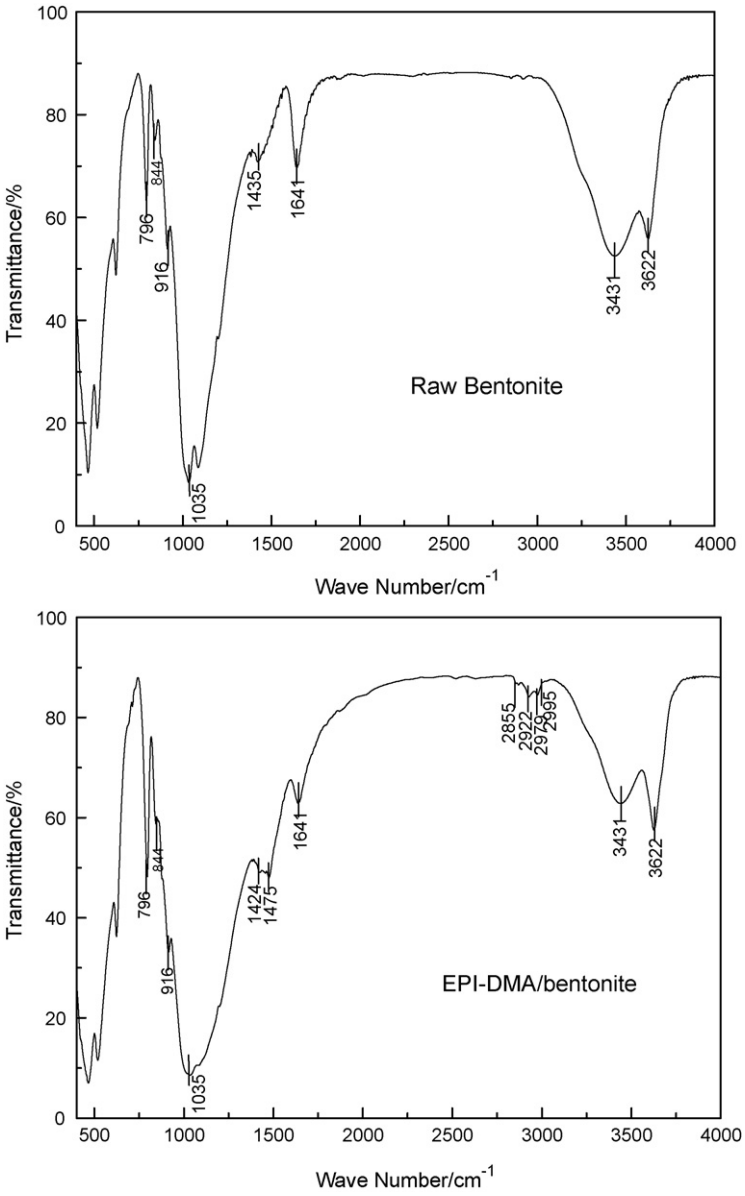

Fig. 2. FTIR spectra of raw bentonite and EPI-DMA/bentonite.

where C_0 and C_e are the initial and equilibrium concentrations (mg/L), respectively, V is the volume of dye solution (mL) and W is the weight (g) of EPI-DMA/bentonite adsorbent.

3. Results and discussion

3.1. Characteristics of EPI-DMA/bentonite

3.1.1. XRD analysis of EPI-DMA/bentonite

The XRD patterns of raw and EPI-DMA/bentonite were recorded. The 2θ peaks for raw and EPI-DMA/bentonite were 7.23° and 5.96° and the calculated basal spacing of the two samples were 12.54 Å and 15.22 Å, respectively, which indicated that the basal spacing of bentonite expanded from 12.54 Å to 15.22 Å due to the loading of EPI-DMA. This observation suggested that EPI-DMA molecules intercalated into the interlayers of bentonite and the interlayer space was extended.

3.1.2. C/N analysis of EPI-DMA/bentonite

The ratio of C/N for raw bentonite and EPI-DMA/bentonite from elemental analysis results was 0 and 4.96, respectively; and the calculated value of C/N ratio for EPI-DMA was 5.14, which confirmed that the intercalation of EPI-DMA molecules between the bentonite layers occurred, and these results were also consistent with FTIR results.

3.1.3. FTIR analysis of EPI-DMA/bentonite

To identify the functional groups present in raw bentonite and EPI-DMA/bentonite adsorbent and provide evidence for modification achieved through EPI-DMA treatment, FTIR analysis of raw bentonite and EPI-DMA/bentonite has been conducted, as shown in Fig. 2.

The FTIR results confirm that the reaction of EPI-DMA molecules between the bentonite layers occurred: the bands between 2855 and 2995 cm^{-1} were only observed for EPI-DMA/bentonite. They could be attributed to the symmetric and asymmetric stretching vibrations of the methyl and methylene groups. The bands at

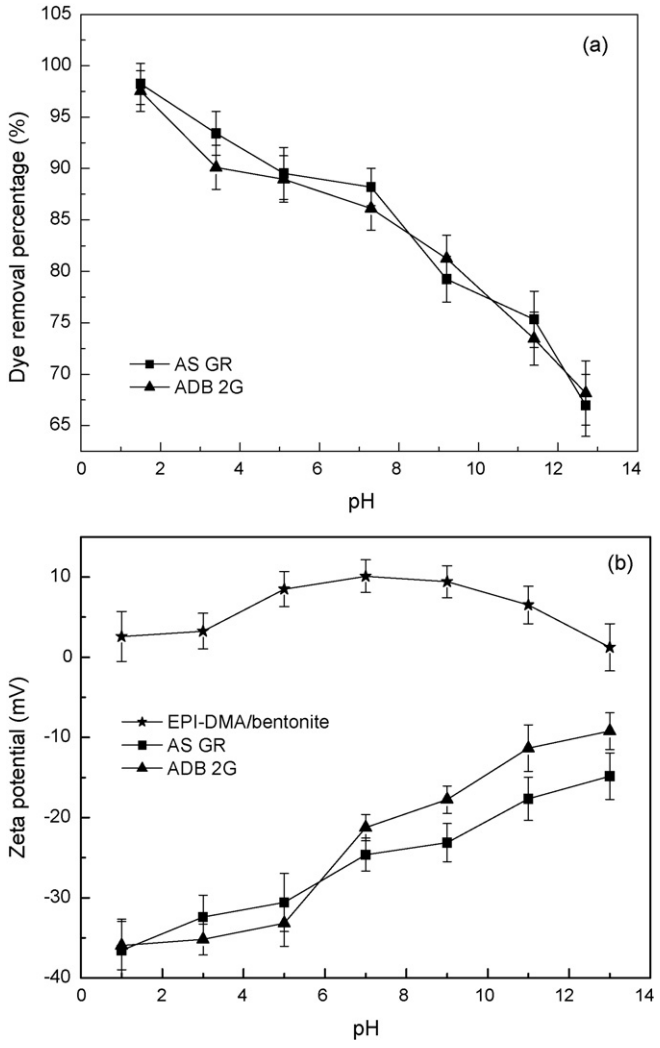

Fig. 3. Effect of solution pH on the dyes removal efficiency (a) and the zeta potential of EPI-DMA/bentonite and acid dyes (b). Experimental conditions: dye solution concentration 50 mg/L, adsorbent dosage 0.2 g/100 mL, salt concentration 0 M, adsorption time 2.0 h, and temperature 303 K.

3431, 3622 and 1641 cm^{-1}, which resulted from the OH deformation of water, were observed in both raw bentonite and EPI-DMA/bentonite, but the peak intensity of EPI-DMA/bentonite was lower than that of raw bentonite. This may be acceptable evidence for the increased hydrophobic nature of the bentonite surface due to the EPI-DMA polymer addition.

3.2. Effect of solution pH

To study the influence of solution pH on the adsorption capacities of EPI-DMA/bentonite for acid dyes, experiments were carried out using various initial pHs varying from 1 to 13. From Fig. 3(a), it is observed that the adsorption was highly dependent on the pH of the solution, and indicated that the acid dye removal efficiencies decreased with the increase of solution pH.

The $-SO_3^-$ groups are characteristic structure of acid dyestuff. The dye bears strong negative charge [32] whereas the EPI-DMA/bentonite maintains a net positive charge in solution, which was also verified by the zeta potential measurement (as shown in Fig. 3(b)). Thereby a significantly high electrostatic attraction exists between the positively charged amidocyanogens of EPI-DMA/bentonite and the negatively charged dyes, thus causing the dye adsorption [19,21,28,32].

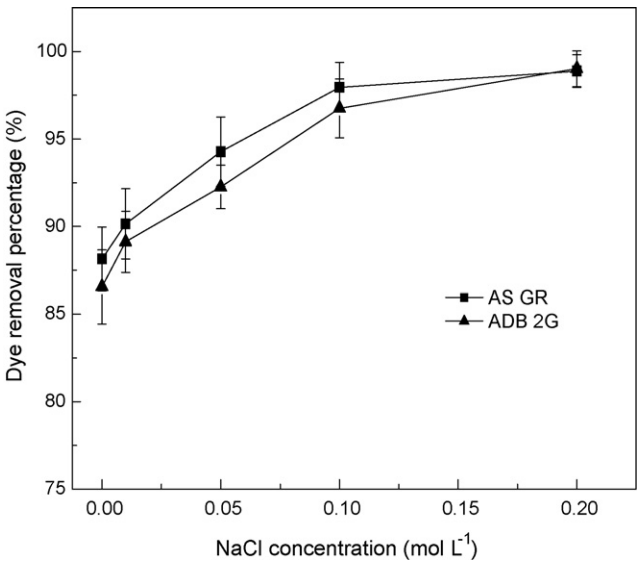

Fig. 4. Effect of NaCl concentration on dyes removal efficiency. Experimental conditions: dye solution concentration 50 mg/L, adsorbent dosage 0.2 g/100 mL, initial solution pH, adsorption time 2.0 h, and temperature 303 K.

At lower pHs, more protons would be available, thereby a significantly high electrostatic attraction existed between the positively charged adsorption sites and negatively charged dye anions, which caused the enhanced dye adsorption [28,32]. But as the solution pH increased, besides the decrease of negative charge of reactive dyes, the positive charge of adsorbent surface also decreased due to the abundance of OH^-, which can weaken the reaction of dye and EPI-DMA/bentonite and thereby causing a decrease in adsorption.

3.3. Effect of salt concentration

The effects of NaCl with different concentrations ranging from 0.01 M to 0.2 M on the dye removal efficiencies of EPI-DMA/bentonite for both dyes are shown in Fig. 4. It is observed that the variation of NaCl concentration exhibited a significant effect on dyes adsorption and high salt concentration was contributive to dye removal. The presence of salt in wastewater led to high ionic strength, which may significantly affect the performance of the adsorption process [33], and the facilitation for dyes adsorption could be produced by two mechanisms [34,35]: one is the addition of salts resulting in the minimization of the repulsion among the negatively charged functional groups of dyes. With the addition of NaCl, the intermolecular forces between dye molecules, such as van der Waals forces, ion–dipole forces and dipole–dipole forces increased and consequently the repulsion forces among the negatively charged functional groups of dyes decreased, which resulted in the dimerization of dyes in solution, rendering the molecule smaller and more hydrophobic, and it was favorable for adsorption process. The other mechanism is the increase of ionic strength causing the compression of the diffuse double layer on the adsorbent, which facilitated the electrostatic attraction and contributed to the adsorption consequently. Some other researchers also reported about similar mechanism for the effect of salt on the adsorption [34,36,37].

3.4. Adsorption isotherms

Analysis of adsorption isotherms is important for developing a model that can be used for adsorption process design, and the isotherms obtained under different temperatures can provide basic data for thermodynamics study to deduce adsorption mechanism.

Table 1
Parameters obtained from Langmuir and Freundlich models.

Acid dye	Langmuir parameter			
	T (K)	Q_0 (mg/g)	K_L (L/mg)	r_L^2
AS GR	293	42.19	1.76	0.947
	303	45.54	1.07	0.880
	313	51.79	1.29	0.957
ADB 2G	293	34.34	1.24	0.955
	303	35.93	2.31	0.944
	313	40.78	2.27	0.937
Acid dye	Freundlich parameter			
	T (K)	$1/n$	K_F [(mg/g)(L/mg)]	r_F^2
AS GR	293	0. 223	15.23	0.993
	303	0.232	21.32	0.985
	313	0.248	25.90	0.992
ADB 2G	293	0. 188	20.58	0.989
	303	0.200	23.27	0.993
	313	0. 246	25.14	0.995

In the present work, the results obtained from the equilibrium adsorption experiments, at the temperatures of 293, 303 and 313 K and at the dye solution initial pH, were analyzed according to the most frequently employed models Freundlich and Langmuir isotherms:

$$Q_e = K_F C_e^{1/n} \tag{2}$$

$$Q_e = \frac{Q_0 K_L C_e}{1 + K_L C_e} \tag{3}$$

And the linear forms of these models are as follows, respectively

$$\ln\ Q_e = \ln K_F + \frac{1}{n} \ln C_e \tag{4}$$

$$\frac{1}{Q_e} = \frac{1}{Q_0} + \left(\frac{1}{Q_0 K_L}\right) \frac{1}{C_e} \tag{5}$$

where C_e is the adsorbate equilibrium concentrations in the liquid (mg/L); Q_e is the adsorbate equilibrium amount in solid phases (mg/g); Q_0 is the maximum adsorption capacity according to Langmuir monolayer adsorption (mg/g); K_L is constant according to the Langmuir model (L/mg); K_F (mg/g)(L/mg) and n is Freundlich constant related to adsorption capacity and adsorption intensity of the adsorbent, respectively. The values of K_F and $1/n$ can be obtained from the intercept and slope, respectively, of the linear plot of experimental data of $\ln Q_e$ versus $\ln C_e$. And the values of Q_0 and K_L can be calculated from the slope and intercept of the linear plot of $1/Q_e$ versus $1/C_e$. The adsorption isotherms for AS GR and ADB 2G onto EPI-DMA/bentonite are shown in Fig. 5 and the calculated parameters are listed in Table 1.

Based on the correlation coefficient as shown in Table 1, Freundlich equation represents a better fit of experimental data than Langmuir, in all cases. It indicates that the surface of EPI-DMA/bentonite is mainly made up of heterogeneous adsorption patches [38] in addition to less homogeneous patches [9]. Freundlich constant, n, is a measure of adsorption intensity. As seen from Table 1, the values of $1/n$ for both dyes were below 1 at all the experimental temperatures, which indicate high adsorption intensity [39]. The Freundlich constant, K_F, which are related to the adsorption capacity, also shows that the adsorption capacity increased with temperature increase, indicating that the adsorption processes are endothermic in nature. But the increase of the values of $1/n$ with the temperature increase suggests the decreasing trend of the adsorption intensity. As temperature increased, the more dye molecules were adsorbed, the keener the competitions for the limited adsorption sites and the stronger the repulsions among the molecules, which resulted in decrease of adsorption intensity.

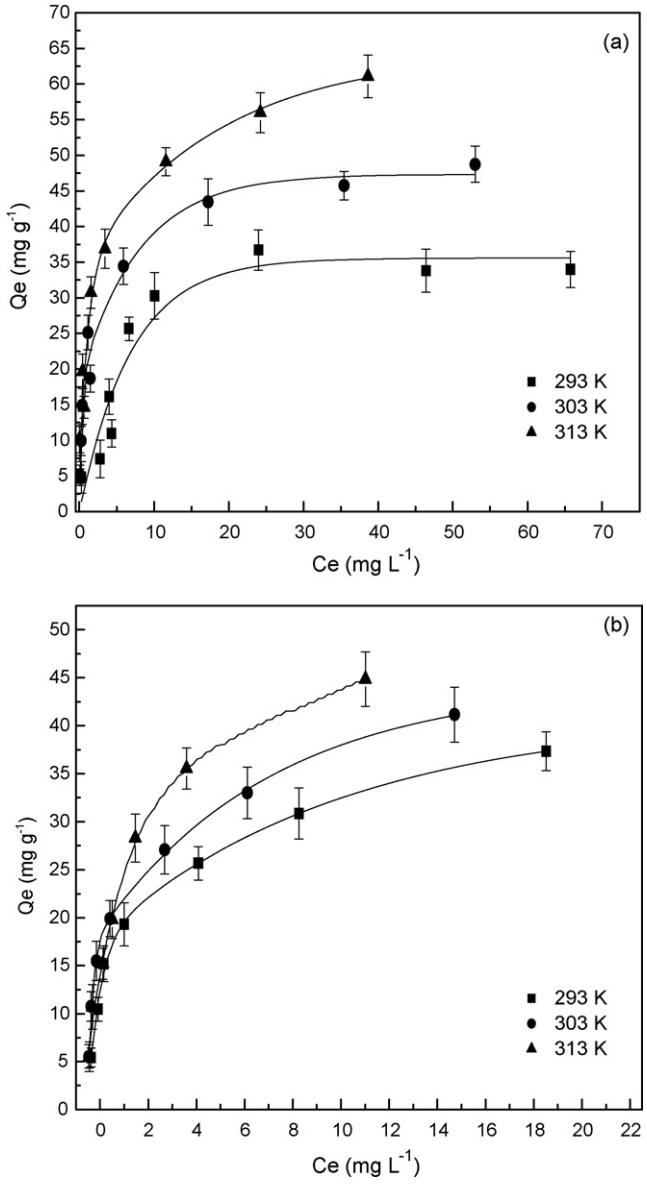

Fig. 5. Isotherms for acid dyes adsorption onto EPI-DMA/bentonite at different temperatures: (a) AS GR and (b) ADB 2G. Experimental conditions: adsorbent dosage 0.2 g/100 mL, initial solution pH, salt concentration 0 M, and adsorption time 2.0 h.

To compare the adsorption capacity of different bentonite adsorbent towards the two acid dyes with that of EPI-DMA/bentonite, three bentonite adsorbents were selected: raw bentonite, cationic surfactant-cetyltrimethylammonium bromide (CTMAB) modified bentonite (CTMAB/bentonite) and cationic polymer-polydiallydimethylammonium (PDMDAAC) modified bentonite (PDMDAAC/bentonite). Take the experiment at 303 K for example. For Acid Scarlet (AS GR), the adsorption capacity of raw bentonite, CTMAB/bentonite and PDMDAAC/bentonite was 4.12 mg/g, 30.28 mg/g and 42.72 mg/g, respectively; and for Acid Dark Blue 2G (ADB 2G), the adsorption capacity was 3.67 mg/g, 24.85 mg/g and 33.34 mg/g, respectively. Whereas, the adsorption capacity of EPI-DMA/bentonite for AS GR and ADB 2G was 45.54 mg/g and 35.93 mg/g, respectively. From the results, it can be concluded that the adsorption capacity of EPI-DMA/bentonite was higher than the other three bentonite based adsorbent. So, EPI-DMA/bentonite has advantages in acid dye removal.

Table 2
Thermodynamic parameters for adsorption of both dyes onto EPI-DMA/bentonite.

Acid dye	T (K)	K_s	$r^2_{K_s}$	ΔG^0 (kJ mol^{-1})	ΔH^0 (kJ mol^{-1})	ΔS^0 (J mol^{-1} K^{-1})
AS GR	293	1422	0.970	−17.68	23.39	140.19
	303	1967	0.968	−19.11		140.25
	313	2626	0.986	−20.49		140.17
ADB 2G	293	1039	0.982	−16.92	26.04	146.62
	303	1415	0.998	−18.28		146.27
	313	2059	0.997	−19.86		146.64

3.5. Thermodynamic study

The thermodynamic parameters, including the free energy changes (ΔG^0), standard enthalpy changes (ΔH^0) and the entropy changes (ΔS^0) associated with the adsorption process, can be used to deduce the adsorption mechanism. They can be calculated by the dependence of thermodynamic equilibrium constant (K_s) on temperatures [40,41]:

$$\Delta G^0 = -RT \ln K_s \tag{6}$$

$$\ln K_s = -\frac{\Delta H^0}{RT} + \frac{\Delta S^0}{R} \tag{7}$$

The thermodynamic equilibrium constant (K_s) for the adsorption of AS GR and ADB 2G on EPI-DMA/bentonite can be calculated using the equation [42]:

$$K_s = \frac{Q_e}{C_e} \cdot \frac{\nu_1}{\nu_2} \tag{8}$$

where Q_e and C_e reflect the same parameters as described in the Langmuir and Freundlich equation, ν_1 is the activity coefficient of the adsorbed solute, and ν_2 is the activity coefficient of the solute in equilibrium suspension. The ratio of activity coefficients was assumed to be uniform in the dilute range of the solutions [42]. As the concentration of the dye in the solution approached zero, the activity coefficient approached unity and Eq. (8) became

$$\lim_{C_e \to 0} \frac{Q_e}{C_e} = K_s \tag{9}$$

The values of K_s are obtained by plotting $\ln Q_e/C_e$ versus C_e and extrapolating to $C_e = 0$ [42–44]. The calculated values of K_s and the correlation coefficients are listed in Table 2.

According to Eq. (6), the values of ΔG^0 were calculated and listed in Table 2. The values of ΔG^0 of dye–EPI-DMA/bentonite adsorption systems are all negative, which indicates the spontaneous adsorption processes. Moreover, the increase in the absolute value of ΔG^0 with increasing temperature indicates that higher temperatures facilitated the adsorption.

The value of ΔH^0 and ΔS^0 can be calculated from the slope and intercept of the van't Hoff plot (Eq. (7)) of $\ln K_s$ against $1/T$, respectively, and the results are listed in Table 2. The positive value of ΔH^0 indicates that the adsorptions of both dyes onto EPI-DMA/bentonite are endothermic. When attraction between adsorbates and an adsorbent took place, the change in standard enthalpy was caused by various forces, including van der Waals, hydrophobicity, hydrogen bonds, ligand exchange, dipole–dipole interactions and chemical bonds [45]. According to the magnitude of different forces, the nature of physical or chemical adsorption can be identified by the sum of different forces. Generally, the magnitude of standard enthalpy changes for absolute physical adsorption is less than 20 kJ mol^{-1}, while chemisorption is in the range of 80–200 kJ mol^{-1} [46]. In this study, the enthalpies implied by the temperature dependence were 23.39 and 26.04 kJ mol^{-1}, respectively for AS GR and ADB 2G adsorption, suggesting that both acid dyes adsorption processes should be regarded as between physical adsorption and chemisorption but dominated by physical adsorption, since the enthalpy change was a little higher than 20 kJ mol^{-1}. So, this may be the reason why the dye adsorption capacities increased with temperature rise and the adsorption is not chemisorption in nature.

In addition, the positive standard entropy change (ΔS^0) value implies that in the dye–EPI-DMA/bentonite adsorption system, although the adsorption process caused an entropy decrease for the adsorbed dye molecules, the entropy increase of dye molecules in dissolved state due to rising temperature was much greater, and consequently the ΔS^0 of the whole adsorption system increased. So the entropy increase of dye molecules in the dissolved state was another factor contributing to the dye adsorption onto EPI-DMA/bentonite.

3.6. Adsorption process design analysis

Batch adsorption process design can be predicted by using the adsorption isotherms [24]. A schematic diagram of a multi-stage batch adsorption system is shown in Fig. 6.

The starting inflow containing V (L) of solution and an initial dye concentration C_0 (mg/L) entered the first batch adsorber with an adsorbent amount W_1 (g) with Q_0 (mg/g) loading of initial dye. After reaching adsorption equilibrium and then separation, the V (L) solution with dye concentration C_1 (mg/L) entered the second adsorber with an adsorbent with W_2 (g) and Q_0 (mg/g) dye loading to be adsorbed and separated again, and so on. The solution concentration of the effluent from each adsorber became C_i (mg/L). The dye loading on the adsorbent for each stage increased from Q_0

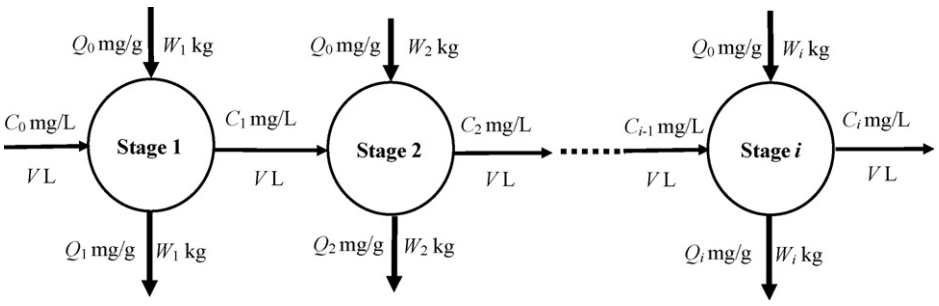

Fig. 6. Multi-stage batch adsorption process for dye removal.

to Q_i (mg/g). When fresh adsorbent was used, $Q_0 = 0$, and the mass balance at each stage in a multi-stage adsorption system can be expressed as:

$$V(C_{i-1} - C_i) = W_i(Q_i - Q_0) = W_i Q_i \tag{10}$$

where i is the sequence number of adsorption stage ($i = 1, 2, 3, \ldots, m$). When the adsorption comes to equilibrium, C_i is the dye solution equilibrium concentration at the ith stage, W_i and Q_i are the adsorbent amount and the dye equilibrium loading on the adsorbent, respectively, at the ith stage, namely $C_i = C_{ei}$ and $Q_i = Q_{ei}$. According to the previous study, the relation of C_e and Q_e obeyed the Freundlich equation well, so the adsorption equilibrium at ith stage is

$$Q_i = K_F C_i^{1/n} \tag{11}$$

Combining Eqs. (10) and (11), the following is obtained:

$$C_{i-1} - C_i = \frac{W_i Q_i}{V} = \frac{W_i K_F C_i^{1/n}}{V} \tag{12}$$

The total amount of dye removal can be evaluated as follows:

$$\sum_{i=1}^{m}(C_{i-1} - C_i) = \sum_{i=1}^{m}\frac{W_i K_F C_i^{1/n}}{V} \tag{13}$$

The dye removal percentage in each adsorption stage, R_i, can be calculated from the equation:

$$R_i = \frac{C_{i-1} - C_i}{C_0} = \frac{W_i K_F C_i^{1/n}}{V C_0} \tag{14}$$

So, the total dye removal percentage is obtained from the following equation:

$$\sum_{i=1}^{m} R_i = \frac{K_F}{V C_0}\sum_{i=1}^{m} W_i C_i^{1/n} \tag{15}$$

For the ith stage, the relation of C_i and C_0 can be represented as:

$$C_i = \left(1 - \sum_{j=1}^{i} R_j\right) C_0 \tag{16}$$

and substituting it into Eq. (15) we obtain:

$$\sum_{i=1}^{m} R_i = \frac{K_F}{V C_0}\sum_{i=1}^{m} W_i \left[\left(1 - \sum_{j=1}^{i} R_j\right) C_0\right]^{1/n} \tag{17}$$

Using Eqs. (14), (16) and (17), the removal percentage of dye at any given initial dye concentration can be predicted and the adsorbent amount needed for multi-stage systems can also be evaluated.

If the solution is treated using a number of batch adsorption stages rather than a single-stage batch, the efficiency of solute removal can be improved [47]. Analytically, if the total solute removal efficiency is fixed, an increased number of stages in the multi-stage adsorption process reduce the adsorbent consumption. A typical example is considered for the case of a two-stage batch adsorption, where the treated dye solution volume is 10 m^3 and the initial dye concentration entering the first stage is 50 mg/L. At Stage 1 of the two-stage batch adsorption system, a series of added amounts of the adsorbent, namely EPI-DMA/bentonite, from 1 kg up to 20 kg (1 kg increment), has been supposed. So, each system numbered from 1 to 20 is based on a 1 kg adsorbent amount interval at Stage 1 of the two-stage adsorption system. For the system numbered N, the adsorbent amount in the first stage W_1, is

$$W_1 = 1\,\text{kg} + (N-1) \times 1\,\text{kg} = N\,\text{kg} \tag{18}$$

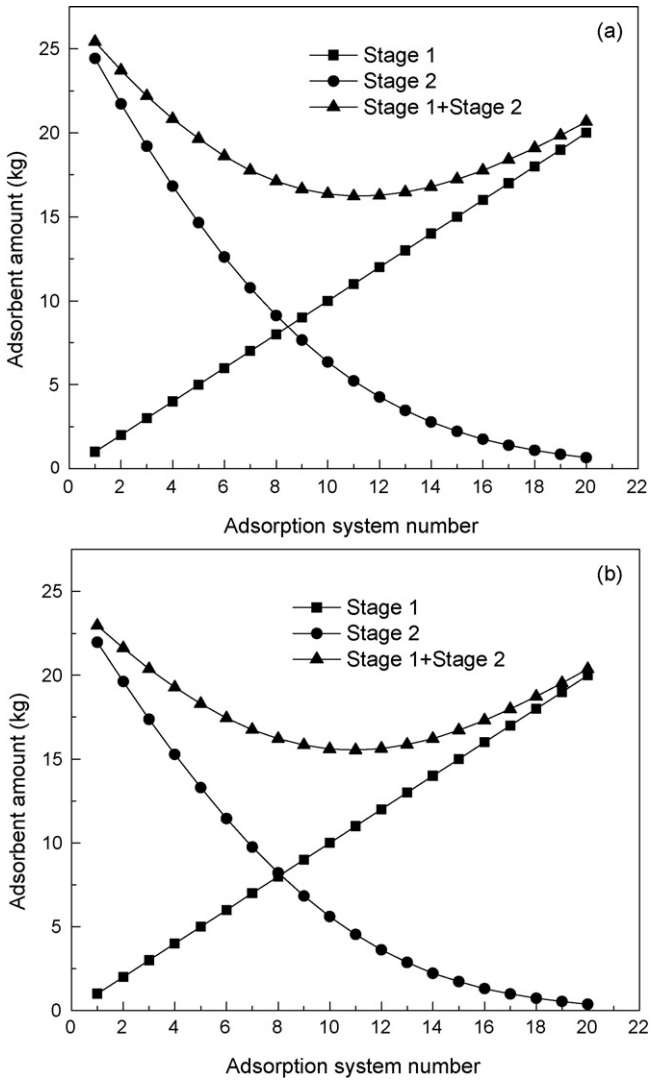

Fig. 7. Adsorbent amount needed for each stage in two-stage adsorption process for 99% dye removal: (a) AS GR and (b) ADB 2G. Conditions: dye solution concentration 50 mg/L, solution volume 10 m^3, initial solution pH, salt concentration 0 M, adsorption time 2.0 h, and temperature 303 K.

where N is the system number ranging from 1 to 20. Take system numbered 5 for example. It indicates that in this two-stage adsorption system, the adsorbent amount in the first adsorber is 1 kg + (5 − 1) × 1 kg = 5 kg.

Then the dye removal efficiency at the first stage (R_1) for each two-stage adsorption system can be determined by Eqs. (14) and (16). Consequently, the adsorbent amount needed in the second stage W_2 can be calculated using Eq. (17), for a fixed total percentage of dye removal. And the total adsorbent amount needed for each two-stage adsorption system, W_{total}, is expressed as:

$$W_{total} = W_1 + W_2 \tag{19}$$

For a fixed percentage of dye removal, the W_{total} values are plotted against the system number, N, and the minimum total adsorbent amount needed for the adsorption system to achieve the fixed dye removal percentage can be determined by the dashed line.

In the two-stage batch adsorption process of EPI-DMA/bentonite for dye removal at a fixed percentage of 99%, the data of adsorbent amount can be plotted for the $N = 20$ systems for Stage 1, Stage 2 and Stage 1 + Stage 2 as shown by the three curves in Fig. 7, and the minimum total EPI-DMA/bentonite amount for 99% dye removal can be identified. A comparison of

Table 3
Minimum total EPI-DMA/bentonite amount needed to achieve various percentages of dye removal for a series of two-stage and a single-stage adsorption systems.

Acid dye	Dye removal percentage	Two-stage adsorption process				Single-stage adsorption process
		System number	W_1 (kg)	W_2 (kg)	W_{total} (kg)	Adsorbent amount (kg)
AS GR	85% dye removal	6	6.00	4.67	10.67	12.50
	90% dye removal	7	7.00	4.85	11.85	14.50
	95% dye removal	9	9.00	4.51	13.51	18.00
	99% dye removal	11	11.00	5.23	16.23	27.30
	99.9% dye removal	14	14.00	5.16	19.16	46.94
ADB 2G	85% dye removal	6	6.00	4.65	10.65	12.20
	90% dye removal	7	7.00	4.75	11.75	14.00
	95% dye removal	9	9.00	4.24	13.24	17.00
	99% dye removal	11	11.00	4.54	15.54	24.40
	99.9% dye removal	14	14.00	3.87	17.87	39.10

the EPI-DMA/bentonite amount needed for five percentages of dye removal, namely 85, 90, 95, 99 and 99.9%, for the two-stage batch adsorption process (Stage 1 + Stage 2) is shown in Fig. 8. The values of minimum total EPI-DMA/bentonite amount needed for the five dye removal percentages are respectively listed in Table 3. Moreover, the EPI-DMA/bentonite amounts needed in a single-stage adsorption process for the same dye removal percentages have been evaluated and also presented in Table 3 to compare with those of two-stage adsorption process.

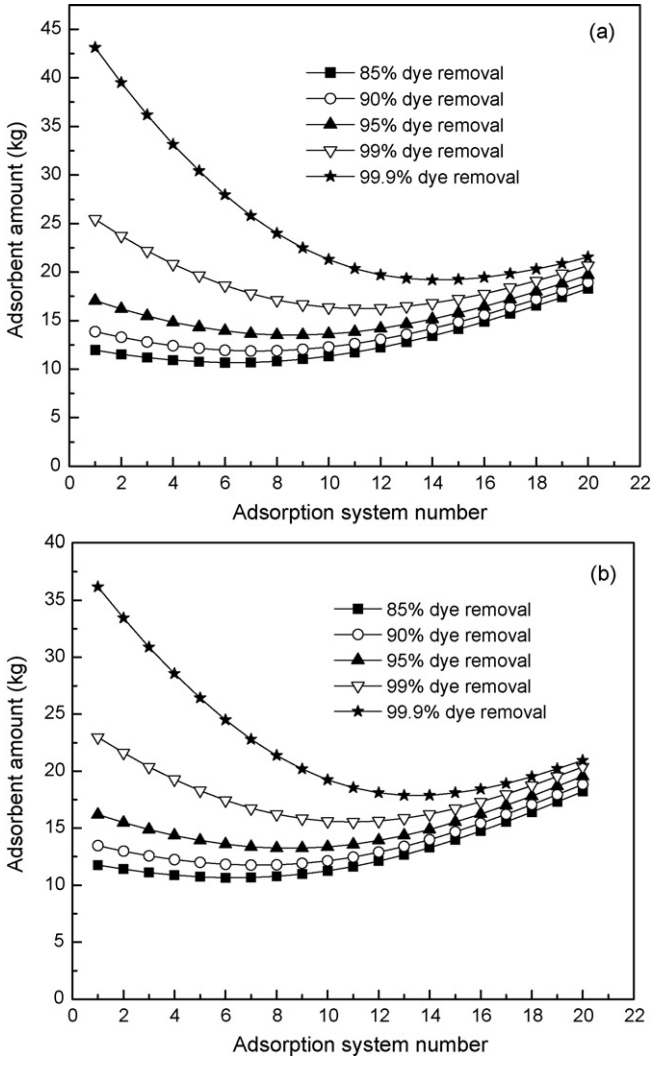

Fig. 8. Minimum total adsorbent amount needed in two-stage adsorption process for various percentages of dye removal: (a) AS GR and (b) ADB 2G. Conditions: dye solution concentration 50 mg/L, solution volume 10 m^3, initial solution pH, salt concentration 0 M, adsorption time 2.0 h, and temperature 303 K.

As can been seen, for both acid dyes, in order to achieve the same percentage of dye removal, two-stage process needed less adsorbent than the single-stage process. For 99.9% AS GR removal, the total EPI-DMA/bentonite amount needed in a single stage was 46.94 kg, whereas in the two-stage process the minimum amount needed was only 19.16 kg as shown by system 14 with adsorbent amount of 14.00 kg for Stage 1 and 5.16 kg for Stage 2; for 99% AS GR removal, a single-stage process needed 27.30 kg EPI-DMA/bentonite and the two-stage process only needed 16.23 kg as shown by system 11 with adsorbent amount of 11.00 kg for Stage 1 and 5.23 kg for Stage 2, and so on for other AS GR removal percentages. Similar analysis can also be made for ADB 2G. Therefore, it can be concluded that the two-stage batch adsorption process can save more adsorbent especially when the required dye removal percentage is much higher.

4. Conclusion

Equilibrium, thermodynamics and process design were conducted for the adsorption of acid dyes from aqueous solutions onto cationic polymer-loaded bentonite (EPI-DMA/bentonite) to study the adsorption properties, mechanisms and optimal adsorbent amount for dyes removal. The Freundlich isotherm was demonstrated to provide the best correlation for the adsorption of acid dyes onto EPI-DMA/bentonite. The negative ΔG^0 indicates the overall adsorption processes were spontaneous; the positive values of ΔH^0 show that both acid dyes adsorption processes were endothermic in nature and should be regarded as between physical adsorption and chemisorption but dominated by physical adsorption, since the enthalpy change was a little higher than 20 kJ mol^{-1}. The positive ΔS^0 values imply that the entropy increase of dye molecules in the dissolved state due to rising temperature was another factor contributing to the dyes adsorption onto EPI-DMA/bentonite.

To predict the minimum amount of EPI-DMA/bentonite required, a two-stage batch adsorption process design was presented based on the well correlated adsorption isotherm. The minimum adsorbent amount to achieve a fixed dye removal percentage for a given volume of wastewater effluents can be easily evaluated. The two-stage batch adsorption process can save more adsorbent compared to single-stage batch. It is particularly suitable for optimizing the use of adsorbent to minimize capital investment costs and especially when the requirement for dye removal efficiency is very high.

Acknowledgements

The authors are grateful to the support of the Postdoctoral Innovation Fund of Shandong Province (200802020), Foundation for

Young Excellent Scientists in Shandong Province (BS2009NY005), Young scientific and technical star plan in Jinan City (20090215), the 11th Five-Year Plan supported by the National Science and Technology (2006BAJ08B05-2), the Chinese National Foundation of Natural Sciences (50878121), the Hi-Tech Research and Development Program of China (2006AA06Z326).

References

[1] M.J. Iqbal, M.N. Ashiq, Adsorption of dyes from aqueous solutions on activated charcoal, J. Hazard. Mater. B139 (2007) 57–66.
[2] M. Özacar, İ.A. Şengil, Adsorption of reactive dyes on calcined alunite from aqueous solutions, J. Hazard. Mater. 98 (2003) 211–224.
[3] M. Doğan, M. Alkan, Adsorption kinetics of methyl violet onto perlite, Chemosphere 50 (2003) 517–528.
[4] S.Y. Lee, S.J. Kim, Adsorption of naphthalene by HDTMA modified kaolinite and halloysite, Appl. Clay Sci. 22 (2002) 55–63.
[5] Y.S. Ho, G. McKay, Sorption of dye from aqueous solution by peat, Chem. Eng. J. 70 (1998) 115–124.
[6] Y.S. Ho, G. McKay, Kinetic models for the sorption of dye from aqueous solution by wood, Process Saf. Environ. Protect. 76 (1998) 183–191.
[7] M. Akçay, G. Akçaym, The removal of phenolic compounds from aqueous solutions by organophilic bentonite, J. Hazard. Mater. 113 (2004) 189–193.
[8] S.L. Bartelt-Hunt, S.E. Burns, J.A. Smith, Nonionic organic solute sorption onto two organo-bentonites as a function of organic-carbon content, J. Colloid Interface Sci. 266 (2003) 251–258.
[9] A.S. Özcan, B. Erdem, A. Özcan, Adsorption of Acid Blue 193 from aqueous solutions onto BTMA-bentonite, Colloid Surf. A: Physicochem. Eng. Aspects 266 (2005) 73–81.
[10] A. Özcan, Ç. Ömeroğlu, Y. Erdoğan, A.S. Özcan, Modification of bentonite with a cationic surfactant: an adsorption study of textile dye Reactive Blue 19, J. Hazard. Mater. 140 (2007) 173–179.
[11] M. Özacar, İ.A. Şengil, A two stage batch adsorber design for methylene blue removal to minimize contact time, J. Environ. Manage. 80 (2006) 372–379.
[12] C. Breen, R. Watson, Polycation-exchanged clays as sorbents for organic pollutants. Influence of layer charge on sorption capacity, J. Colloid Interface Sci. 208 (1998) 422–429.
[13] G.J. Churchman, Formation of complexes between bentonite and different cationic polyelectrolytes and their use as sorbents for non-ionic and anionic pollutants, Appl. Clay Sci. 21 (2002) 177–189.
[14] C. Breen, The characterisation and use of polycation-exchanged bentonites, Appl. Clay Sci. 15 (1999) 187–219.
[15] T.S. Anirudhan, P.S. Suchithra, P.G. Radhakrishnan, Synthesis and characterization of humic acid immobilized-polymer/bentonite composites and their ability to adsorb basic dyes from aqueous solutions, Appl. Clay Sci. 43 (2009) 336–342.
[16] D. Shen, J. Fan, W. Zhou, B. Gao, Q. Yue, Q. Kang, Adsorption kinetics and isotherm of anionic dyes onto organo-bentonite from single and multisolute systems, J. Hazard. Mater. 172 (1) (2009) 99–107.
[17] J.H. Choi, W.S. Shin, S.H. Lee, Application of synthetic polyamine flocculants for dye wastewater treatment, Sep. Sci. Technol. 36 (13) (2001) 2945–2968.
[18] D.J. Joo, W.S. Shin, S.P. Lee, Effect of polyamine flocculant types on dye wastewater treatment, Sep. Purif. Technol. 38 (2003) 66l–678.
[19] Q.Y. Yue, Q. Li, B.Y. Gao, A.J. Yuan, Y. Wang, Formation and characteristics of cationic-polymer/bentonite complexes as adsorbents for dyes, Appl. Clay Sci. 35 (2007) 268–275.
[20] Q.Y. Yue, Q. Li, B.Y. Gao, Y. Wang, Kinetics of adsorption of disperse dyes by polyepicholorohydrin-dimethylamine cationic polymer/bentonite, Sep. Purif. Technol. 54 (2007) 279–290.
[21] Q. Li, Q.Y. Yue, Y. Su, B.Y. Gao, J. Li, Two-step kinetic study on the adsorption and desorption of reactive dyes at cationic polymer/bentonite, J. Hazard. Mater. 165 (2009) 1170–1178.
[22] A.S. Özcan, B. Erdem, A. Özcan, Adsorption of Acid Blue 193 from aqueous solutions onto Na-bentonite and DTMA-bentonite, J. Colloid Interface Sci. 280 (2004) 44–54.
[23] Q. Kang, W. Zhou, Q. Li, B. Gao, J. Fan, D. Shen, Adsorption of anionic dyes on poly(epicholorohydrin-dimethylamine) modified bentonite in single and mixed dye solutions, Appl. Clay Sci. 45 (4) (2009) 280–287.
[24] M. Özacar, İ.A. Şengil, Equilibrium data and process design for adsorption of disperse dyes onto alunite, Environ. Geol. 45 (2004) 762–768.
[25] S. Chatterjee, Su. Chatterjee, B.P. Chatterjee, A.K. Guha, Adsorptive removal of congo red, a carcinogenic textile dye by chitosan hydrobeads: binding mechanism, equilibrium and kinetics, Colloid Surf. A 299 (2007) 146–152.
[26] W.T. Tsai, C.Y. Chang, C.H. Ing, C.F. Chang, Adsorption of acid dyes from aqueous solution on activated bleaching earth, J. Colloid Interface Sci. 275 (2004) 72–78.
[27] Z. Eren, F.N. Acar, Adsorption of Reactive Black 5 from an aqueous solution: equilibrium and kinetic studies, Desalination 194 (2006) 1–10.
[28] J.J.M. Órfão, A.I.M. Silva, J.C.V. Pereira, S.A. Barata, I.M. Fonseca, P.C.C. Faria, M.F.R. Pereira, Adsorption of a reactive dye on chemically modified activated carbons—influence of pH, J. Colloid Interface Sci. 296 (2006) 480–489.
[29] A. Özcan, E.M. Öncü, A.S. Özcan, Adsorption of Acid Blue 193 from aqueous solutions onto DEDMA-sepiolite, J. Hazard. Mater. 129 (2006) 244–252.
[30] B.H. Hameed, D.K. Mahmoud, A.L. Ahmad, Equilibrium modeling and kinetic studies on the adsorption of basic dye by a low-cost adsorbent: coconut (*Cocos nucifera*) bunch waste, J. Hazard. Mater. 158 (2008) 65–67.
[31] Ö. Demirbaş, M. Alkan, M. Doğan, The removal of victoria blue from aqueous solution by adsorption on a low-cost material, Adsorption 8 (2002) 341–349.
[32] A.S. Özcan, A. Özcan, Adsorption of acid dyes from aqueous solutions onto acid-activated bentonite, J. Colloid Interface Sci. 276 (2004) 39–46.
[33] T.S. Anirudhan, M. Ramachandran, Surfactant-modified bentonite as adsorbent for the removal of humic acid from wastewaters, Appl. Clay Sci. 35 (2007) 276–281.
[34] X. Peng, Z. Luan, H. Zhang, Montmorillonite-Cu(II)/Fe(III) oxides magnetic material as adsorbent for removal of humic acid and its thermal regeneration, Chemosphere 63 (2006) 300–306.
[35] X.S. Wang, Y. Zhou, Y. Jiang, C. Sun, The removal of basic dyes from aqueous solutions using agricultural by-products, J. Hazard. Mater. 157 (2008) 358–374.
[36] G. Alberghina, R. Bianchini, M. Fichera, S. Fisichella, Dimerization of Cibacron Blue F3GA and other dyes: influence of salts and temperature, Dyes Pigments 46 (2000) 129–137.
[37] Y.S. Al-Degs, M.I. El-Barghouthi, A.H. El-Sheikh, G.M. Walker, Effect of solution pH, ionic strength, and temperature on adsorption behavior of reactive dyes on activated carbon, Dyes Pigments 77 (2008) 16–23.
[38] Z Aksu, D. Dönmez, A comparative study on the biosorption characteristics of some yeasts for Remazol Blue reactive dye, Chemosphere 50 (2003) 1075–1083.
[39] W.T. Tsai, C.W. Lai, K.J. Hsien, Effect of particle size of activated clay on the adsorption of paraquat from aqueous solution, J. Colloid Interface Sci. 263 (2003) 29–34.
[40] M. Afzal, F. Mahmood, M. Saleem, Thermodynamics of adsorption of acetone on activated carbon supported metal adsorbent, Colloid Polym. Sci. 270 (1992) 917–929.
[41] M. Saleem, M. Afzal, F. Mahmood, A. Ali, Surface characterization and thermodynamics of adsorption of Pr, Nd, and Er on alumina from aqueous solution, Adsorption Sci. Technol. 9 (1992) 17–29.
[42] V.K. Gupta, P. Singh, N. Rahman, Adsorption behavior of Hg(II), Pb(II), and Cd(II) from aqueous solution on Duolite C-433: a synthetic resin, J. Colloid Interface Sci. 275 (2004) 398–402.
[43] A.A. Khan, R.P. Singh, Adsorption thermodynamics of carbofuran on Sn (IV) arsenosilicate in H^+, Na^+ and Ca^{2+} forms, Colloid Surf. 24 (1987) 33–42.
[44] A. Demirbas, A. Sari, O. Isildak, Adsorption thermodynamics of stearic acid onto bentonite, J. Hazard. Mater. B 135 (2006) 226–231.
[45] B. von Oepen, W. Kördel, W. Klein, Sorption of nonpolar and polar compounds to soils: processes, measurements and experience with the applicability of the modified OECD-Guideline 106, Chemosphere 22 (1991) 285–304.
[46] B Gu, J. Schmitt, Z. Chen, L. Liang, J.F. McCarthy, Adsorption and desorption of natural organic matter on iron oxide: mechanisms and models, Environ. Sci. Technol. 28 (1994) 38–46.
[47] M. Özacar, Contact time optimization of two-stage batch adsorber design using second-order kinetic model for the adsorption of phosphate onto alunite, J. Hazard. Mater. B 137 (2006) 218–225.